The Mechanism of Self-Sustained Electron Emission from Magnesium Oxide

DIETRICH DOBISCHEK, HAROLD JACOBS, AND JOHN FREELY
Signal Corps Engineering Laboratories, Fort Monmouth, New Jersey
(Received March 2, 1953)

Thin films of magnesium oxide, under the influence of an electric field, have been observed to emit extremely large secondary emission currents when bombarded with electrons. This current has been found to be exponentially dependent upon the electric field in the oxide film, and under certain conditions, to persist for many hours after the bombarding current has been cut off. Experiments have shown that the enhanced emission is due to the fact that the surface acquires a positive charge during bombardment, thereby creating an intense field in the thin film. Electrons released in the film by internal ionization are then accelerated by the field and cause further ionization, so that eventually an electron avalanche ensues. It has been found that there are two components of the enhanced electron emission. The first component is a true field-enhanced secondary emission effect similar to that described in previous work. The second component is a self-sustained electron emission. This self-sustained electron emission is produced by the same type of avalanche effect, except that the internal ionization of the dielectric is initiated by electrons produced from within the material rather than by electrons bombarding the material from an external source.

I. INTRODUCTION

IN the work previously reported by the authors,[1] thin films of MgO were observed to emit extremely large secondary emission currents when bombarded with electrons. These currents were found to be exponentially dependent upon the electric field. The conclusion was made that the oxide acquires a positive charge during bombardment, thereby creating an intense electric field in the thin film. Electrons released in the film by internal ionization are then sufficiently accelerated by the field so as to cause further ionization, and eventually an electron avalanche takes place within the oxide in a manner similar to the Townsend effect in gas discharges.

In more recent experiments which are herein described, it was found that the secondary emission current became increasingly independent of the bombarding current when higher fields were applied within the oxide film. At these high fields, the secondary emission was often several thousand times larger than the primary current, and usually persisted for many hours even when the primary current was turned off. Therefore, it was concluded that this self-sustained emission must be initiated by a source other than the primary electrons. Experiments were then devised to separate the self-sustained emission from the avalanche current initiated by the primary electrons. In addition a determination was made of the oxide surface potential, the electric field within the oxide, and the dependence of the secondary and self-sustained emission upon this field. Finally the rise times for surface charging were measured.

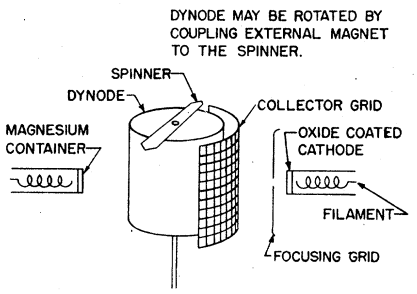

FIG. 1. Experimental tube.

[1] Jacobs, Freely, and Brand, Phys. Rev. 88, 492 (1952).

II. THE DEPENDENCE OF SECONDARY EMISSION UPON PRIMARY CURRENT. THE SELF-SUSTAINED EMISSION. THE DEPENDENCE OF SELF-SUSTAINED EMISSION UPON THE ELECTRIC FIELD

Experimental tubes were constructed as shown in Fig. 1. MgO films were deposited on the dynode in the manner described in the previous work.[1] Using the static test circuit of Fig. 2 measurements were made of the secondary emission current as a function of primary current, at a constant difference in potential between collector and dynode (ΔV). These tests were repeated for several different constant ΔV's. From these data, the ratio of secondary to primary current was determined as a function of primary current at different constant ΔV's. The results are shown in Fig. 3, and it can be seen that at lower values of ΔV (up to 110v) the ratio of secondary to primary current remains constant for varying bombarding currents, i.e., the secondary emission current is completely dependent upon the primary

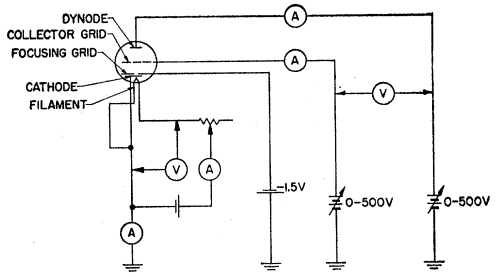

FIG. 2. Static test circuit.

current. However, at higher ΔV's the ratio of secondary to primary current is no longer constant for different bombarding currents, which means that the secondary emission becomes increasingly independent of the bombarding current. Furthermore, it was observed that in the region of high ΔV the secondary emission current may persist for many hours even when the bombarding current was turned off. Therefore, it is apparent that in this region of field an initiating source other than the bombarding electrons is causing the emission. When after shutting off the cathode the self-sustained emission was measured as a function of ΔV, it was also found to increase exponentially with increasing ΔV, as shown in Fig. 4. Thus, the assumption may be made that the self-sustained emission is an avalanche effect too. The total electron emission will now be considered to consist of two electron avalanches, one initiated by bombarding electrons from outside the dielectric, the other initiated by electrons generated within the material.

III. THE SEPARATION OF THE PRIMARY AVALANCHE AND SELF-SUSTAINED EMISSION

In order to separate these two effects the following experiment has been devised. The magnesium oxide film was bombarded as before, and a given potential difference (ΔV) was applied between dynode and collector. The total secondary emission current was then measured, after which the cathode was shut off and measurements made of the self-sustained emission which remained. This self-sustained emission is evidently the avalanche current initiated by electrons generated within the material, while the current which disappears (e.g., total secondary emission current minus the self-sustained emission) is the avalanche current initiated by the primary beam. When these readings were repeated for various values of ΔV, then a measure was obtained of the total secondary emission, the primary avalanche current, and the self-sustained emission current, all as a function of ΔV. This data is shown in Fig. 5. It can be seen that at low values of ΔV the total current is almost exclusively due to the primary avalanche. The self-sustained emission begins at higher fields and increases more rapidly with field than does the primary avalanche, so that at still higher fields the total current is mostly due to the self-sustained emission. This explains why the total secondary emission current becomes increasingly independent of the primary current at higher ΔV's. An interesting effect occurs if the field is increased still further; the self-sustained emission begins to increase almost discontinuously so that an arc occurs. This effect evidently corresponds to the phenomenon of dielectric breakdown.

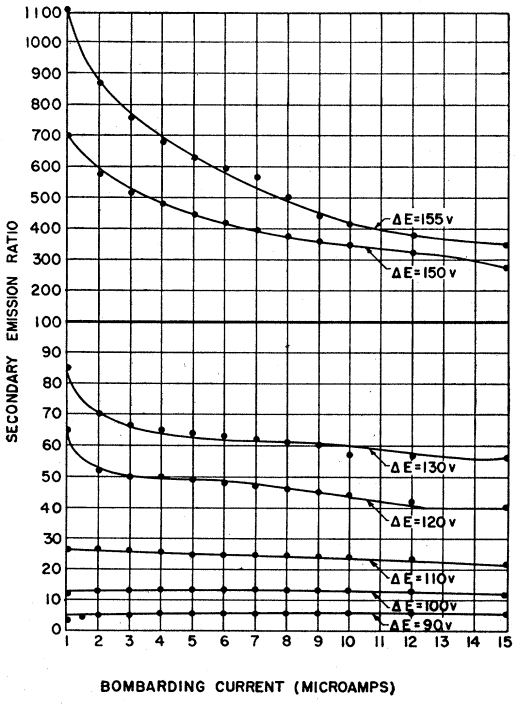

FIG. 3. Secondary emission ratio as a function of bombarding current at various differences in potential between collector and dynode.

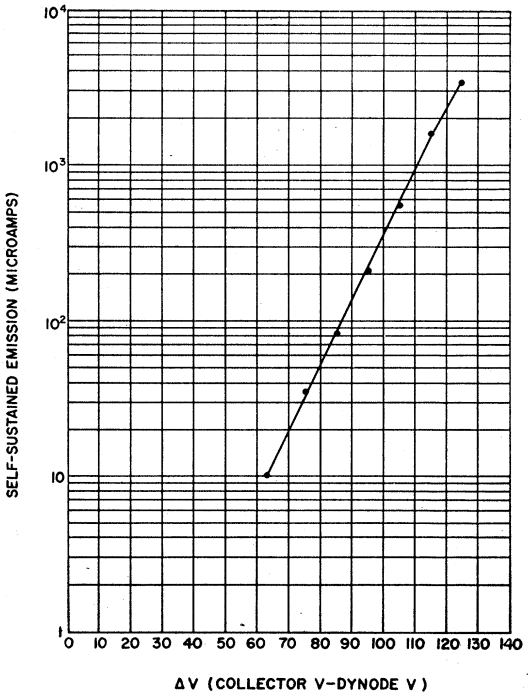

FIG. 4. Log of the self-sustained emission as a function of the difference in potential between collector and dynose.

IV. DETERMINATION OF THE SURFACE POTENTIAL

Since all the tests were made with secondary emission ratios greater than one and since the resistivity of the material was high, the surface of the magnesium oxide layer would tend to charge positively, and, neglecting initial velocity effects, an equilibrium will be established in which the potential of the oxide surface equals the potential of the collector.

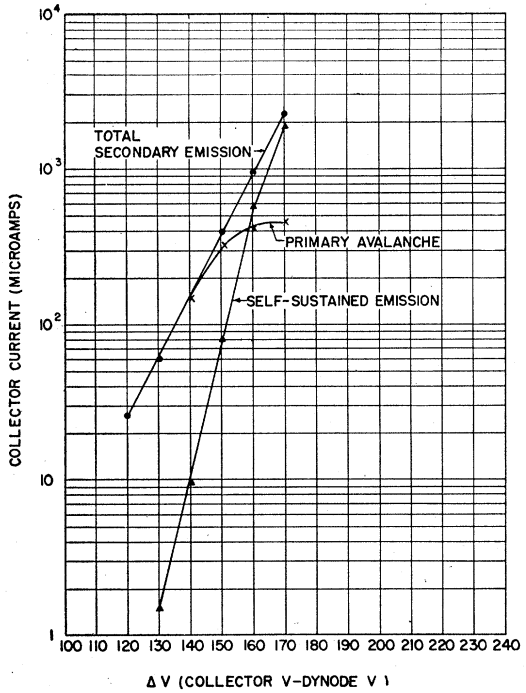

FIG. 5. Log of the total secondary emission, primary avalanche and self-sustained emission as a function of the difference in potential between collector and dynode.

This picture is not strictly true however, since some of the surface charges will recombine and the true equilibrium will be established with the surface at a somewhat lower potential than the collector grid. The rate of recombination will thereby determine the potential difference between the surface and collector. After equilibrium has been established the current leaving the film equals the current entering. As will be explained in a later section, this latter current is the sum of the primary current and the current entering the film from the dynode base metal. In order to determine the true potential at the surface for a given collector potential, the following experiments have been devised.

It was observed that for a constant ΔV, the total secondary emission current increased linearly as the collector grid was moved closer to the oxide surface. Therefore, a tube was constructed with a movable collector grid, and measurements were made of the total secondary emission *versus* ΔV for various distances of the collector grid from the dynode. Simultaneous readings were also taken of the primary avalanche and self-sustained emission *versus* ΔV in the manner described previously. Figure 6 shows the variation of the total secondary emission with collector spacing, while Figs. 7 and 8 show the variation of primary avalanche and self-sustained emission currents at various distances of collector to dynode. From Fig. 6, ΔV was plotted *versus* distance (collector to dynode) for a constant total secondary emission current. It was found that as the distance decreases, the ΔV needed to obtain this given current also decreases. This plot was repeated for several different currents as in Fig. 9, and it was found that in all cases the potential difference ΔV required to

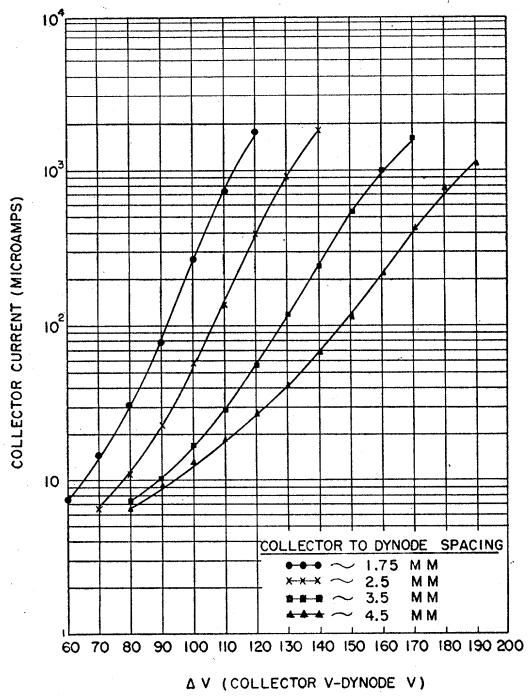

FIG. 6. Log of the total secondary emission *vs* ΔV for various distances of collector to dynode.

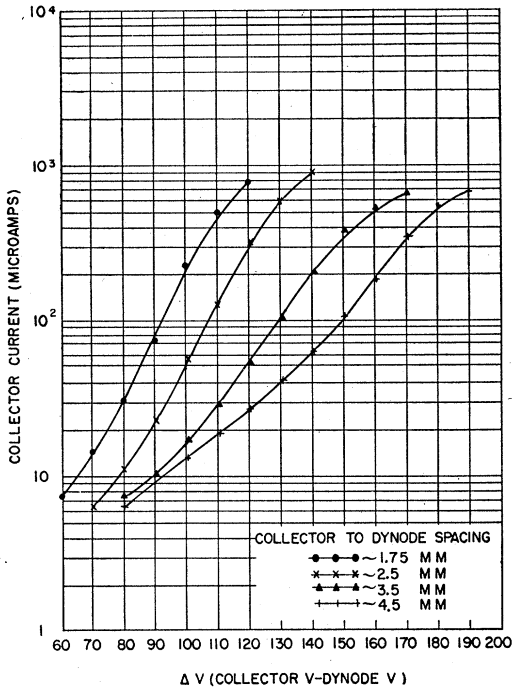

FIG. 7. Log of the primary avalanche current *vs* ΔV for various distances of collector to dynode.

obtain a given total secondary current decreased linearly as the collector was brought closer to the dynode. Since ΔV varied linearly with grid spacing, these constant current lines were easily extrapolated to zero distances. This effectively gave the surface potential, with respect to the dynode, for a given total secondary emission current. If plots were then made of these various constant currents *versus* the corrected ΔV (or the true potential difference across the oxide film) as in Fig. 10, the true variation of the total secondary emission with ΔV could be determined. Furthermore, since the film was found to be 10^{-4} cm thick,[1] the actual variation of the total secondary emission with the electric field in the oxide film could be obtained. From

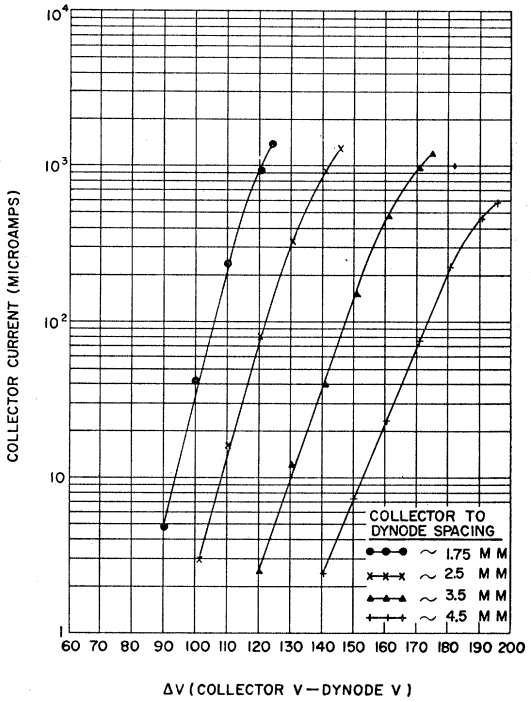

FIG. 8. Log of the self-sustained emission *vs* ΔV for various distances of collector to dynode.

the data in Figs. 7 and 8, a plot was made of the collector-to-dynode distance *versus* ΔV for constant primary avalanche current and also for constant self-sustained emission current. This was repeated as before for several constant currents of both avalanches, and again the constant currents were extrapolated to zero distance as in Figs. 11 and 12 to find the true ΔV required to obtain these currents. Finally, in Fig. 13 the primary avalanche current and the self-sustained emission current were plotted *versus* these true ΔV's. Hence a determination has been made of the actual electric field in the film and of the dependence of the total secondary emission, primary avalanche current, and self-sustained emission current on this field.

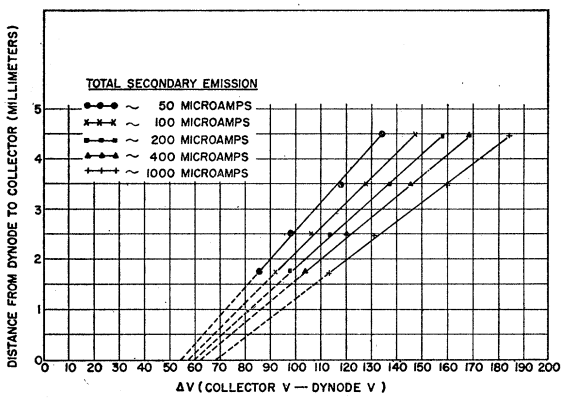

FIG. 9. The ΔV required to draw a given total secondary emission current as a function of the distance between dynode and collector.

V. SURFACE CHARGING AND RECOMBINATION

The previous sections have shown that the total field enhanced secondary emission is caused by an intense

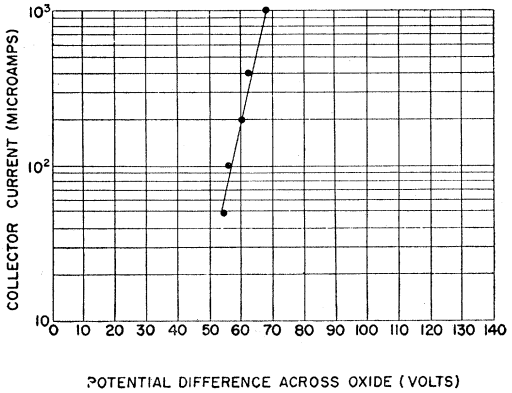

FIG. 10. Log of the total secondary emission as a function of the potential difference across the oxide film.

electric field in the magnesium oxide film. Therefore, the formation of the positive surface charges which set up this electric field will now be discussed.

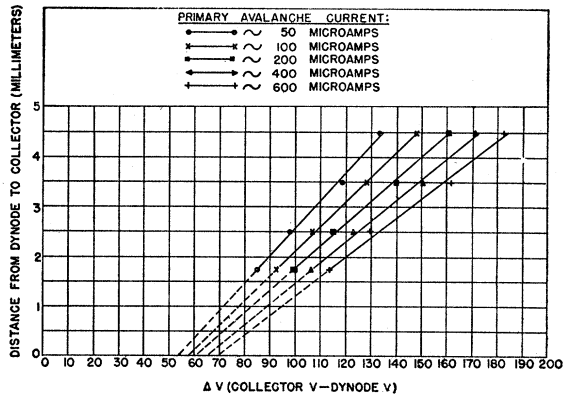

FIG. 11. The ΔV required to draw a given primary avalanche current as a function of the distance between dynode and collector.

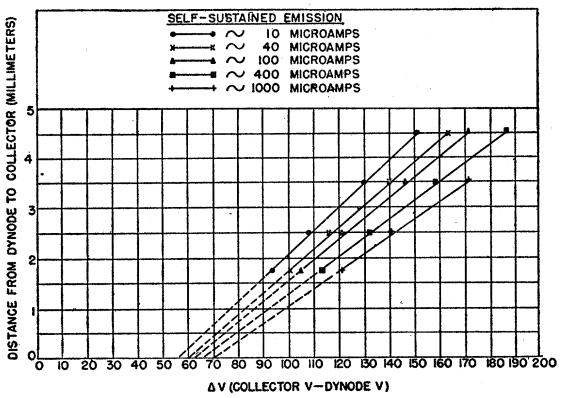

FIG. 12. The ΔV required to draw a given self-sustained avalanche current as a function of the distance between dynode and collector.

A. Surface Charging by Small Self-Sustained Emission Currents

An excellent insight into the equilibrium between charging and recombination may be gained by observing the behavior of small self-sustained emission currents as a function of time. In this experiment the oxide film was bombarded with a small current (< one microamp) and the difference in potential between collector and dynode was increased until a measurable self-sustained avalanche current was detected. The cathode was then shut off, and with ΔV kept constant the self-sustained emission current was measured as a function of time for several different ΔV. Figure 14 shows the data from this experiment. At low values of ΔV (170 and 180 volts) the self-sustained emission current decreased with time, at higher ΔV (200 and 210 volts) it initially increased with time, later reaching an equilibrium where the current remained fairly constant. Finally when ΔV's as high as 240 volts were used, the current increased very rapidly with time, terminating in an arc, after which the current dropped abruptly to zero.

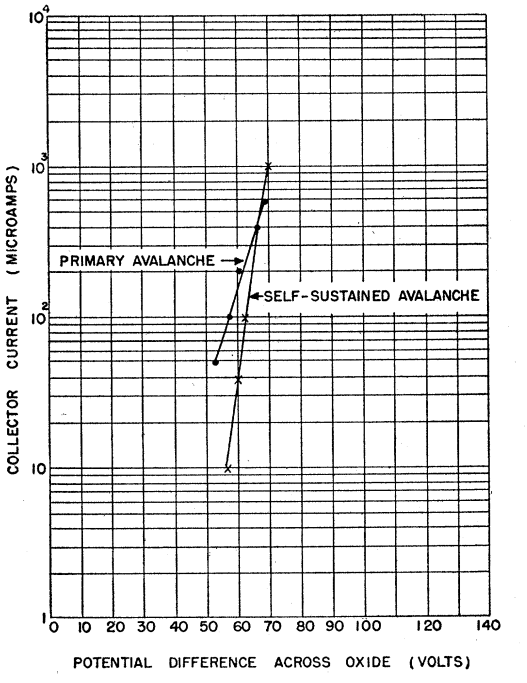

FIG. 13. Log of the primary avalanche and the self-sustained avalanche as a function of the potential difference across the oxide film.

These observations indicate that at low ΔV's the rate of recombination was greater than the rate of ionization so that an equilibrium was never reached. When higher ΔV's were applied, the rate of ionization was initially higher than the rate of recombination so that the current increased. This increase continued until the surface potential became approximately equal to the collector potential after which the current remained constant. The equilibrium current was higher for higher ΔV's and consequently the time to reach equilibrium was longer in these cases. When finally ΔV was increased still further, the rate of ionization was again greater than the rate of recombination. Now, however, ΔV was sufficiently high so that the field in the oxide built up to the point where dielectric breakdown occurred. This results in an arc which completely discharges the surface and causes the current to drop to zero. Therefore no equilibrium could be established in this case.

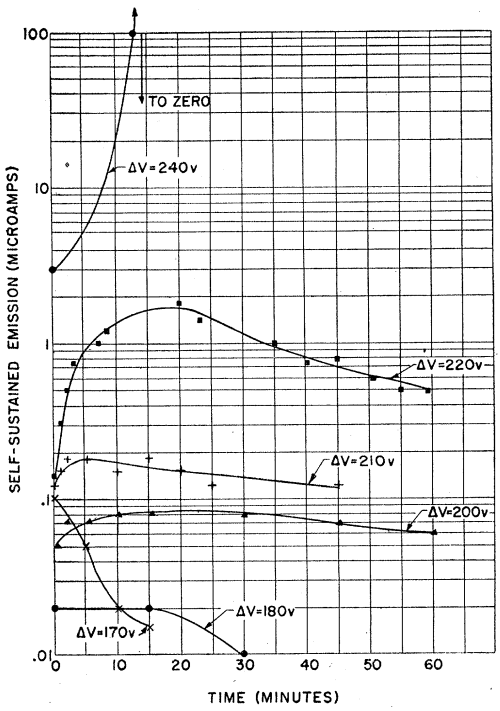

FIG. 14. Self-sustained emission *vs* time for various ΔV's.

B. Effects of Bombarding Energy

Another experiment which casts some light on the problem of surface charging is one in which the collector and dynode were placed at the same potential (i.e., no field in the MgO) while measurements were made of the primary current during variations in the bombarding energy. The results are shown in Fig. 15, and it can be seen that the primary current increased very slowly with increasing bombarding energy until a critical point was reached after which the primary current increased very rapidly. This is attributed to the fact that at the lower bombarding energies the surface of the film acquires a negative charge since the secondary emission ratio is less than one. This negative charge inhibits the primary current from the cathode so that as the bombarding energy is increased the cathode current shows almost no increase. As the bombarding energy is increased still further, a point is reached at which the secondary emission ratio becomes just greater than one. The surface will then suddenly acquire a positive charge which will greatly enhance the primary emission. Further increases in bombarding energy will cause the surface to charge even more positively, and consequently the primary emission will continue to increase.

TABLE I. Variations of α with field (volts/cm).

F volts/cm	α
7.56×10^5	2.81×10^4
8.20×10^5	3.50×10^4
8.58×10^5	4.19×10^4
9.14×10^5	4.90×10^4
9.71×10^5	5.30×10^4

VI. INTERPRETATIONS AND CONCLUSIONS

A. Dependence of α on Field

In the experimental work described above it was shown that the total field-enhanced secondary emission is made up of two components, the primary avalanche current and the self-sustained emission. In a previous paper the primary avalanche was described as being similar to the Townsend effect in a gas discharge. The expression for the primary avalanche is, in this case,

$$i=i_0e^{\alpha x}, \tag{1}$$

where i is the total current, i_0 is the bombarding current, α is the number of electrons created per centimeter of path per incident electron, and x is the depth of penetration of the incident electrons into the oxide. In the present work a determination has been made of the dependence of the primary avalanche current upon the true surface potential of the magnesium oxide. Therefore an estimation of the electric field in the oxide may be made in the following manner. Dielectric breakdown

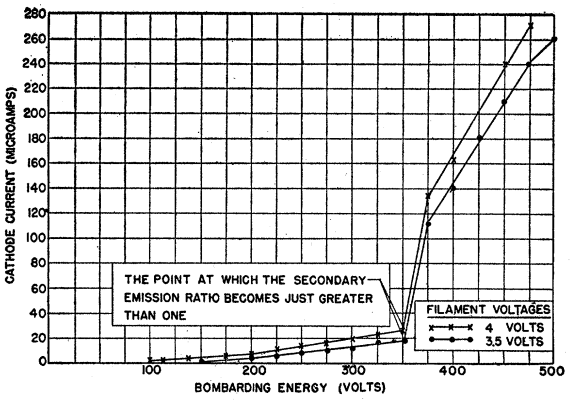

FIG. 15. Cathode current as a function of bombarding energy.

is known to occur at a field of 10^6 volts per centimeter. Since in the present experiments breakdown has been found to occur at a surface potential of 70 volts with respect to the base plate (see Fig. 13), the assumption may be made that this potential difference across the thin film corresponds to a field of 10^6 volts per cm. Then, lower voltages were assumed to represent proportionately lower fields. Now α may be determined as a function of field from the data in Fig. 13 by using Eq. (1). The distance x in this case may be estimated to be 10^{-4} cm as determined in previous experiments. In Table I there are listed values of α at different fields, and for convenience Fig. 16 is given to show the dependence of α upon field in this particular region.

B. Dependence of γ on Field

In a Townsend discharge, with an initiating source in addition to the primary beam, the total current may be written as

$$i=i_0e^{\alpha x}/[1-\gamma(e^{\alpha x}-1)], \tag{2}$$

where i_0 is the bombardment current and γ is the ratio of initiating electrons to electrons released by secondary processes. The electrons liberated in these secondary

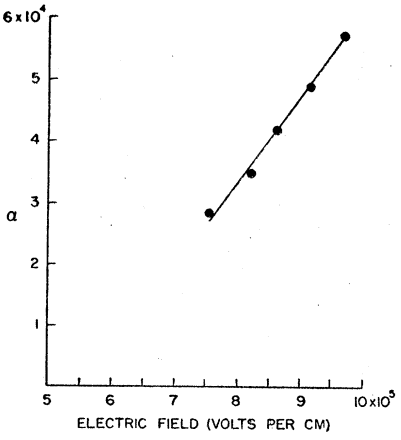

FIG. 16. Variation of α with field.

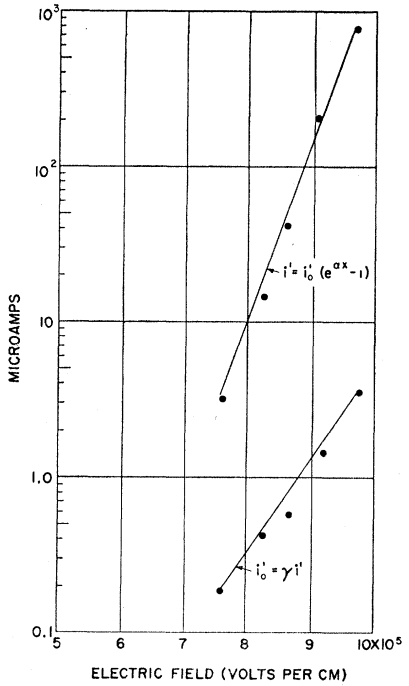

FIG. 17. Variation of self-sustained emission i' and self-initiating current i_0' with field.

processes continue on to form additional avalanches. When the denominator of (2) goes to zero, the discharge becomes self-sustained. Therefore, the condition necessary for this to occur is that

$$\gamma=(e^{\alpha x}-1)^{-1}. \tag{3}$$

We may now extend the gas-discharge analogy further so as to include the phenomenon of self-sustained emission in magnesium oxide. In this case i in Eq. (2) represents the total secondary emission, $i_0e^{\alpha x}$ is the primary avalanche current, and γ is the ratio of new initiating electrons formed per positive ion on the surface. In addition, it should be pointed out that the number of new ions formed on the surface exactly equals the number of electrons measured at the collector grid. The ratio γ can then be represented as i_0'/i', where i_0' is the number of new initiating electrons per second appearing from within the oxide, and i' is the total self-sustained emission.

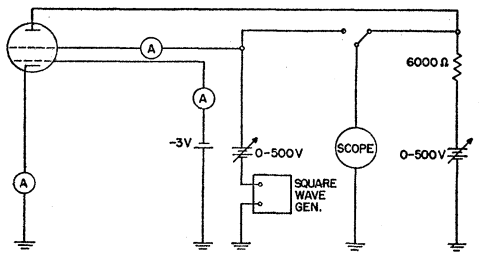

FIG. 18. Dynamic test circuit.

The condition for self-sustained emission in magnesium oxide can then be represented by

$$\gamma=i_0'/i'=(e^{\alpha x}-1)^{-1}, \tag{4}$$

and since α is a function of field we should find that γ is also a function of field.

By means of Fig. 13, we can find the values of the self-sustained emission current i', and from Table I the value of α for each particular field is determined. Substituting these values in Eq. (4), γ and i_0' can be obtained as a function of field. The values determined in this manner are listed in Table II.

It is of interest to note that γ goes down with increasing fields, as it often does in the case of gas discharges. However, this does not mean that i_0' goes down. In fact i_0' does rise exponentially with field (see Fig. 17), but i' rises at a more rapid rate and hence the ratio γ or i_0'/i' goes down with increasing fields.

C. Discussion of the Role of Field Emission

Since i_0' rises exponentially with field, it might appear that the initiating electrons are liberated from the base metal into the pores of the magnesium oxide

TABLE II. Variations in γ and i_0' with field.

F volts/cm	γ	i_0' μa	i' μa
7.56×10^5	0.064	0.192	3
8.20×10^5	0.031	0.435	14
8.58×10^5	0.0151	0.605	40
9.14×10^5	0.00753	1.506	200
9.71×10^5	0.00500	3.70	740

by field emission. Here, due to the high fields and long mean free paths, the initiating electrons gain enough energy, i.e., 5 to 10 ev, to cause further avalanche effects. Unfortunately, however, the hypothesis that initiating electrons are released by field emission can be shown to be very doubtful. The Fowler-Nordheim equation for field emission is

$$J=C\mathcal{E}^2\exp(D/\mathcal{E})\text{amp/m}^2, \tag{5}$$

in which

$$C=\frac{6.2\times10^{-6}}{E_B}\left(\frac{E_M}{E_W}\right)^{\frac{1}{2}}\text{amp/volt}^2, \tag{6}$$

$$D=6.8\times10^9(E_W)^{\frac{3}{2}}, \tag{7}$$

$\mathcal{E}$ is the field in volts/meter, E_W is the work function, E_M is the Fermi level of the electrons in the base metal, and E_B is the sum of the Fermi energy level and the work function. It should be noted that E_W is the work function of the base metal as the electrons travel from the metal into the empty pores of the magnesium oxide. This is equivalent to stating that the electrons travel by field emission from the base metal to a vacuum. If the hypothesis is correct, upon determining

TABLE III. Comparison of calculated and observed rise times under various conditions of testing.

Test number	Calculated rise time (seconds)	Observed rise time (seconds)	Type of emission	j_c at start of pulse (amp/cm²)	Frequency of square wave field cycles/second	Amplitude of square wave in volts
1	0.72×10^{-3}	1.25×10^{-3}	Secondary emission	7.5×10^{-5}	200	20
1	0.56×10^{-3}	1.25×10^{-3}	Self-sustained emission	10.0×10^{-5}	200	20
2	1.8×10^{-4}	3.1×10^{-4} sec	Secondary emission	2.7×10^{-4}	800	20
2	1.8×10^{-4}	2.1×10^{-4} sec	Self-sustained emission	2.8×10^{-4}	800	20
3	8.3×10^{-5}	8.35×10^{-5}	Secondary emission	6.0×10^{-4}	4000	20
3	8.3×10^{-5}	6.25×10^{-5}	Self-sustained emission	5.75×10^{-4}	4000	20
4	5.2×10^{-5}	5.0×10^{-5}	Secondary emission	6.0×10^{-4}	5000	13

E_W by variations of i_0' with field, we should find E_W to be in the order of magnitude of 2.5 to 5.0 electron volts.

Substituting the values of i_0' at particular values of $\mathcal{E}$ taken from Table II, and solving the simultaneous equations, we can determine the value of E_W. When this procedure was carried out, E_W was found to be approximately 0.3 ev. The hypothesis therefore leads to a value of the work function which is too small by a factor of ten, and this concept of the mechanism for the liberation of the new initiating electrons should probably be abandoned. At the present time it is felt that the mechanism for the creation of the i_0' current might be the result of a photoelectric effect in which photons are ejected during the recombination of positive ions and electrons. Some of these photons penetrate into the oxide and liberate new electrons into pores of the magnesium oxide structure. These new electrons then travel with long mean free paths and under the influence of high fields, initiate new avalanches. As a rough estimate, one electron might be generated per thousand photons as is known from the work on photoelectric emission. The ratio γ has been found not to differ from this value too markedly. Further experiments probably should be carried out to check the validity of this hypothesis.

Another group of electrons to be considered are the replenishment electrons, or the recombination electrons. These are electrons liberated from the base metal into the conduction band of the magnesium oxide by Fowler-Nordheim field emission. Here they drift relatively slowly with mean free path $\sim10^{-8}$ cm until they reach the surface and recombine with the positive charges located in this region. In equilibrium, the current leaving the dielectric must equal the current entering. If we substitute the values of i' into Eq. (5), we obtain a work function E_W of 0.4 to 0.5 ev. This value does seem somewhat reasonable if we assume that the magnesium oxide has traps in its forbidden zone. Such values have been determined for the work function of BaO—SrO mixtures in oxide-coated cathodes. Therefore, it appears that the field-emitted electrons serve rather to recombine with the positive charges and cannot initiate avalanches because of their short mean free paths and low energies.

VII. RISE-TIME MEASUREMENTS

It has been shown that the self-sustained emission is similar in mechanism to the primary avalanche current. The only fundamental difference between the two effects is that the primary avalanche is initiated by the bombarding electrons, while the self-sustained emission is initiated by electrons generated within the dielectric. If the two processes are as similar as has been postulated, then the charging process should be the same in both cases, and the rise times for surface charging should be found to be equal. Furthermore both effects should exhibit rise times in agreement with McKay's formula for the charging time of an insulator. This equation may be written as

$$t=8.85\times10^{-14}EK/j_p(\delta-1) \text{ seconds}, \tag{8}$$

where t is the time in seconds, E is the increase in the field across the dielectric, j_p is the primary current density, δ is the secondary emission ratio, and K is the dielectric constant. A slight modification can be made here if it is realized that $j_p(\delta-1)$ is approximately the current (j_c) which is collected. Consequently Eq. (8) becomes

$$t=8.85\times10^{-14}EK/j_c. \tag{9}$$

Experiments were then performed to check the agreement of experimental rise times with the theoretical values predicted by McKay. Simultaneously these measurements allowed a comparison to be made between the rise times obtained for primary avalanche current and for self-sustained emission.

The circuit used in these tests is shown in Fig. 18. A square-wave variation of voltage was applied on the collector grid. This effectively produced a variation of the field in the dielectric since the oxide surface charges to approximately the grid potential. The variation of field was superimposed on a constant field already present in the dielectric. Time lags were measured for secondary emission both with and without bombarding current. The measurements made with bombardment current applied were taken in a region of field where very little self-sustained emission was noted, so that the results obtained were representative of the primary avalanche current alone. On the other hand, the self-sustained emission was measured in a field region where the total secondary emission is almost completely self-sustained. For purposes of comparison, approximately equal currents were used in both cases.

The rise times were observed by placing an oscilloscope across a 10 000Ω resistor in the plate circuit. The voltage loss across the plate resistor was subtracted

from the amplitude of the square wave to obtain the variation of potential across the dielectric. The change in field in the oxide was then estimated in the following manner. It was assumed that approximately 100 volts across a thickness of 10^{-4} cm provided a field of 10^6 volts per centimeter, with smaller fields corresponding to smaller differences in potential. The collector current (j_c) was measured at the beginning of the pulse, and the rise time t was measured directly. These experimental rise times were then computed and compared with the theoretical values found from Eq. (9). As shown in Table III, good agreement was found. Furthermore, it can be seen from Table III that the time lags for similar primary avalanche and self-sustained emission currents were also in good agreement.

It should be noted that there was some difficulty in estimating the area of the emitting region, and therefore the current densities may be off by a factor of three. However the order of magnitude between calculated and experimental values is close. Furthermore it can be seen that where the current density decreased, the rise time increased as predicted by Eq. (9).

Acknowledgment should be made to Dr. John E. Gorham of the Signal Corps Engineering Laboratories for his advice and encouragement during the course of the work.

PHYSICAL REVIEW VOLUME 91, NUMBER 4 AUGUST 15, 1953

Phase Transitions in Antiferroelectric $PbHfO_3$†

GEN SHIRANE* AND RAY PEPINSKY
Department of Physics, Pennsylvania State College, State College, Pennsylvania
(Received May 4, 1953)

Phase transitions in ceramic $PbHfO_3$ have been studied by dielectric and structural measurements. The dielectric constant is about 90 at room temperature, and its temperature dependence shows a small anomaly at 163°C and a pronounced peak of 540 at 215°C. The *P-E* relation, however, is almost linear, showing no ferroelectric hysteresis loops within this temperature range. At room temperature $PbHfO_3$ has a tetragonal lattice of the perovskite type with $a=4.136$A and $c/a=0.991$, and a powder x-ray photograph shows some superstructure lines which have essentially the same character as those of $PbZrO_3$. This shows that $PbHfO_3$ is an antiferroelectric of the $PbZrO_3$ type below 163°C. The crystal structure between 163°C and 215°C is also based on a tetragonal lattice; but the axial ratio c/a is much closer to unity (0.997), and the observed superstructure lines are different from those of the lowest phase. Thus the intermediate phase is another antiferroelectric phase, with a different type of dipole arrangement from that of the lowest phase. At 215°C, it becomes paraelectric, accompanied by a change to a cubic structure.

I. INTRODUCTION

RECENT studies of $PbTiO_3$ [1,2] and $PbZrO$ [3,4] have revealed interesting dielectric properties and relations of these to the crystal structures of these perovskite-type compounds. $PbTiO_3$ is a ferroelectric with a Curie point of 490°C,[2,5] and this is very similar to the much studied Curie point of $BaTiO_3$ [6] at 120°C. The crystal structure[7] of $PbTiO_3$ is distorted to a tetragonal lattice with $c/a=1.063$ below its Curie point. The dielectric properties of $PbZrO_3$, on the other hand, have shown that this crystal is not ferroelectric but antiferroelectric with a Curie point at 230°C, notwithstanding the close resemblance of the permittivity *vs* temperature curve of this crystal to those of $BaTiO_3$ and $PbTiO_3$. The crystal structure[7] of $PbZrO_3$ is distorted to a tetragonal cell, but the axial ratio c/a is less than unity (0.99), in contrast with $BaTiO_3$ and $PbTiO_3$ in which c/a is greater than unity.

No satisfactory explanation has been given of the reason why such an essential difference in dielectric and structural properties can be observed in these very closely related perovskite crystals. Although there is no doubt that the large polarizability of the Pb ion in both compounds contributes to these peculiar phenomena, the essential difference in the compounds is in the ionic radii and polarizabilities of B ions in the ABO_3 type crystals which have Pb as a common A ion. This fact suggests that the further study of lead compounds with different B ions, such as $PbHfO_3$, may give more information about this phenomenon.

Compared with a detailed study of titanates and zirconates of perovskite-type crystals, very little information is available on the properties of hafnates.

† Research conducted under contract with the Air Research and Development Command and with the U. S. Office of Naval Research.
* On leave from Tokyo Institute of Technology, Tokyo, Japan.
[1] G. H. Jonker and J. H. van Santen, Chem. Weekblad **43**, 672 (1947).
[2] G. Shirane and S. Hoshino, J. Phys. Soc. Japan **6**, 265 (1951).
[3] Sawaguchi, Shirane, and Takagi, J. Phys. Soc. Japan **6**, 333 (1951).
[4] Shirane, Sawaguchi, and Takagi, Phys. Rev. **84**, 476 (1951).
[5] H. H. Rogers, Technical Report 56, Laboratory for Insulation Research, Massachusetts Institute of Technology, 1952 (unpublished).
[6] See A. von Hippel, Revs. Modern Phys. **22**, 221 (1950).
[7] H. D. Megaw, Proc. Phys. Soc. (London) **58**, 133 (1946).